On the electron energy loss spectra of small particles

1990 J. Phys.: Condens. Matter 2 7925

(http://iopscience.iop.org/0953-8984/2/39/007)

J. Phys.: Condens. Matter **2** (1990) 7925–7932. Printed in the UK

On the electron energy loss spectra of small particles

R Saniz

Institute of Theoretical Physics, Chalmers University of Technology, S - 412 96 Göteborg, Sweden

Received 7 March 1990

Abstract. Electron energy loss spectroscopy experiments have very recently confirmed that at clean planar metallic surfaces, the smooth decay of the ground-state electronic density induces additional surface modes above the classical one tending to $\omega_p/\sqrt{2}$ for $q \to 0$ (in the non-retarded regime). It is shown here that similar modes—i.e. induced by surface diffuseness, should also be observable in the electron energy loss spectra of small particles of free-electron-like metals. More precisely, these spectra show an additional maximum above the classical modes of a sphere—which are given by $\omega_p/\sqrt{(2l+1)/l}$, $l = 1, \ldots, \infty$—and below ω_p. This maximum is due to the superposition of the contributions of the aforementioned additional modes. Recent experimental reports of the electron energy loss spectra of potassium small particles, showing anomalous modes, can be understood from this point of view.

1. Introduction

Very recently, electron energy loss spectroscopy (EELS) studies of plane metallic surfaces, carried out by Tsuei *et al* [1], have unambiguously confirmed that these systems can sustain multipole surface plasmons in addition to the 'classical' surface mode predicted by Ritchie [2] in 1957. Ritchie predicted this mode applying the hydrodynamic model to a semi-infinite metal in which the electronic ground-state density falls abruptly to zero at the metal/vacuum interface. It was experimentally observed three years later [3]. Thereafter, hydrodynamic models taking into account the smooth decay of the ground-state electronic density at the surface predicted the aforementioned additional modes. For instance, it was shown that the poles of the surface optical absorption density are given by the retarded surface plasmon dispersion relations [4, 5], thus giving an interpretation of the photoemission spectra from Al [6]. Intuitively, one can understand the existence of these modes as follows. In an homogeneous system, the natural oscillation frequency is determined by the density. Since the latter is constant in such a system, there will be a single relevant eigenfrequency in play. In an inhomogeneous system, different parts of the system have different densities and, thus, will tend to oscillate with different frequencies. These oscillations will interfere destructively in general, but it may happen that at certain frequencies, depending on the spatial extension of the inhomogeneous region and the density gradient, they interfere constructively. This would give rise to new collective oscillations, more or less localized in the region of inhomogeneity. (One can guess that this may happen only if the system considered is not too inhomogeneous, i.e. it should present a minimum residual symmetry allowing a well defined extended collective behaviour.)

0953-8984/90/397925+08$03.50

The hydrodynamic model has also been used to study the optical properties of small particles [7, 8]. In [8], the gradual decay of the ground-state electronic density was taken into account. This led, in the dipole approximation, to an additional surface mode at a frequency below the bulk mode ω_p and above the Mie mode $\omega_p/\sqrt{3}$. Unfortunately, the relevant experimental results, demonstrating or ruling out the existence of such a mode, are not readily available. Experiments have often been mainly aimed at measuring the red (or blue) shift of the Mie mode [9], and there are very few reports of the optical absorption spectra ranging from the Mie mode up to ω_p. On the other hand, experiments on these systems are very delicate since the results can be very sensitive to impurities. It is well known that thin overlayers on surfaces give rise to interface modes, which should not be confused with the clean surface ones. (Similar problems may occur in the plane surface case.) From the theoretical point of view, one can point out the time-dependent density functional results of Eckardt [10] for the photoabsorption of small particles. One can see in those results a systematic, more or less broad, maximum above the Mie mode which has not been explicitly identified by their author. For instance, in figures 4 and 5 of the first paper in [10], this maximum is situated between 1.2 and 1.4 ω_s^{cl} (where $\omega_s^{cl} = \omega_p/\sqrt{3}$). This feature can be interpreted as the additional dipolar mode masked by single-particle–hole excitations.

Given the above context, we find most interesting the recent EELS results of vom Felde *et al* [11] on small metallic particles, showing anomalous modes above the classical surface modes of a sphere. In this paper we report our calculations of the EELS spectra of small metallic particles with different radii and for various momentum transfers, showing that those experimental results can be understood in terms of additional surface modes. In section 2, a brief description of the model and the method of calculation is given. Section 3 presents the main results together with a discussion of the conclusions that can be drawn from them.

2. Model and energy loss probability

In the present work, we take a small 'jellium' sphere as a model of a small particle, and describe the electron gas within the hydrodynamic approximation given by

$$\frac{\partial}{\partial t}\boldsymbol{j}(\boldsymbol{r},t) = \frac{\omega_p^2\, n_0(r)}{4\pi}(\boldsymbol{E}(\boldsymbol{r},t) + \boldsymbol{E}^{ext}(\boldsymbol{r},t)) - \gamma \boldsymbol{j}(\boldsymbol{r},t) - \beta^2 \nabla \varrho(\boldsymbol{r},t) \quad (1)$$

where n_0 represents the ground-state electron density (normalized), ω_p is the (bulk) plasma frequency, $\beta^2 = 3v_F^2/5$ (v_F is the Fermi velocity) and γ is a phenomenological damping factor. $\boldsymbol{E}$, $\boldsymbol{j}$ and ϱ are induced fields, and $\boldsymbol{E}^{ext}$ is a perturbing external field (for an account of the hydrodynamic approach see, e.g. [12]). While this does not define the most general hydrodynamic approach (for more general formulations, see [13]), its predictions are qualitatively the same as those of the more general ones (namely, the existence of additional modes induced by surface diffuseness). In the non-retarded case, the system will be completely determined (modulo the boundary conditions) by coupling the above equation with the continuity and the Poisson equations. Following Fujimoto and Komaki [14], we take the sphere centred at the origin and consider an impinging electron following a trajectory given by $\boldsymbol{r}_0(t) = (\boldsymbol{\rho}_0, vt)$, where v is the electron velocity and $\boldsymbol{\rho}_0$ the impact parameter. Hence, the external charge density is given by

$$\varrho_{ext}(\boldsymbol{r}, \boldsymbol{\rho}_0; t) = -e\delta(\boldsymbol{\rho} - \boldsymbol{\rho}_0)\delta(z - vt) \quad (2)$$

($\boldsymbol{r} = (\boldsymbol{\rho}, z)$) and the external potential can formally be written as

$$\phi_{\text{ext}}(\boldsymbol{r}, \boldsymbol{\rho}_0; t) = \int \mathrm{d}^3 r' \frac{1}{|\boldsymbol{r} - \boldsymbol{r}'|} \varrho(\boldsymbol{r}', \boldsymbol{\rho}_0; t). \tag{3}$$

It is readily shown that the work done by the electron in going from $t \to -\infty$ to $t \to +\infty$, given by [14]

$$W(\boldsymbol{\rho}_0) = -e \int_{-\infty}^{+\infty} \mathrm{d}t \, v E_z(\boldsymbol{r}_0(t), \boldsymbol{\rho}_0; t) \tag{4}$$

can be written

$$W(\boldsymbol{\rho}_0) = \frac{\mathrm{i}e}{2\pi v} \int \frac{\mathrm{d}^2 q}{(2\pi)^2} \int \mathrm{d}\omega \, \omega \exp(\mathrm{i}\boldsymbol{q} \cdot \boldsymbol{\rho}_0) \hat{\phi}(\boldsymbol{q}, \omega/v, \boldsymbol{\rho}_0; \omega) \tag{5}$$

where $\hat{\phi}$ stands for the Fourier transform of the induced potential in the variables $\boldsymbol{\rho}$, z and t. Since the diameter of the impinging beam of electrons is actually much bigger than that of the particles themselves, we integrate W over $\boldsymbol{\rho}_0$ to obtain the total work W_{total}. The total energy loss E is given by the real part of W_{total}, and can be expressed as [15]

$$E = \operatorname{Re} W_{\text{total}} = \int \mathrm{d}^2 q \int_0^{\infty} \mathrm{d}\omega \, \hbar\omega P(\boldsymbol{q}, \omega) \tag{6}$$

where $P(\boldsymbol{q}, \omega) = -(e/4\pi^3 v\hbar) \operatorname{Im} \hat{\phi}(\boldsymbol{q}, \omega/v, -\boldsymbol{q}; \omega)$ gives the probability of the electron losing an energy $\hbar\omega$ and changing its momentum by $\hbar\boldsymbol{q}$.

Given a sphere of radius R, the 'surface region' is comprised within an interval $R' < r \leq R$, where $R - R'$ can be of the order of several Å for alkali metals [16]. For $r \leq R'$, we take $n_0(r) = 1$, and for $r > R'$, n_0 is a smooth function decaying to zero at R. In the homogeneous region, the problem has been solved by Tran Thoai and Zeitler [17] and we shall not repeat the calculations here. In the surface region, the problem can be solved using the well known method of 'variation of constants' (see, e.g. Arnold [18]). The formulation is rather straightforward, although the equations are space consuming. Let us just outline the procedure and give the results. In terms of the potential, the system is described by a fourth-order (spatial) differential equation (after having taken the Fourier transform in time). Expanding the fields in terms of spherical harmonics, we are left with the following equation for the radial part

$$\frac{\mathrm{d}^4}{\mathrm{d}r^4} g^l(r) + \nu_3(r) \frac{\mathrm{d}^3}{\mathrm{d}r^3} g^l(r) + \nu_2(r) \frac{\mathrm{d}^2}{\mathrm{d}r^2} g^l(r) + \nu_1(r) \frac{\mathrm{d}}{\mathrm{d}r} g^l(r) + \nu_0(r) g_l(r) = \eta_l(r, Q) \tag{7}$$

with the coefficients and inhomogeneous term given by

$$\begin{aligned}
\nu_3(r) &= \frac{4}{r} \\
\nu_2(r) &= -\frac{2l(l+1)}{r^2} + k^2(r) \\
\nu_1(r) &= \frac{2}{r} k^2(r) - k_s^2 n_0'(r) \\
\nu_0(r) &= \frac{(l+2)(l+1)l(l-1)}{r^4} - \frac{l(l+1)}{r^2} k^2(r) \\
\eta_l(r, Q) &= n_0(r) j_l(Qr) - \frac{n_0'(r)}{Q} j_l'(Qr)
\end{aligned} \tag{8}$$

where $k^2(r) = (\omega^2 + i\omega\gamma - n_0(r)\omega_p^2)/\beta^2$, the j_l are the spherical Bessel functions and $Q^2 = q^2 + \omega^2/v^2$. The final expression for the induced potential in terms of the spherical harmonics reads $\phi(\boldsymbol{r}, \boldsymbol{\rho}_0; \omega) = \sum_{lm} Y_{lm}(\theta, \varphi)\, \phi_{lm}(r, \boldsymbol{\rho}_0; \omega)$, where

$$\phi_{lm}(r, \boldsymbol{\rho}_0; \omega) = 4k_s^2 \frac{e}{v} i^l \int d^2q \, \exp(i\boldsymbol{q}_\parallel \cdot \boldsymbol{\rho}_0) Y_{lm}^*(\theta', \varphi') G_l(r, Q). \tag{9}$$

In the above equation we have introduced the screening length $k_s = \omega_p/\beta$ and the angles θ' and φ' defined by $\boldsymbol{Q} = (\boldsymbol{q}, \omega/v) = (Q, \theta', \varphi')$. The G_l are given by

$$\begin{aligned} G_l(r, Q; \omega) = {} & \tilde{g}_1^l(r; \omega) \left(a_l(\omega) - \int_r^R dr' \, S_{14}^l(r'; \omega) \eta_l(r', Q) \right) \\ & + \tilde{g}_2^l(r; \omega) \int_0^r dr' \, S_{24}^l(r'; \omega) \eta_l(r', Q) \\ & + \tilde{g}_3^l(r; \omega) \left(b_l(\omega) - \int_r^R dr' \, S_{34}^l(r'; \omega) \eta_l(r', Q) \right) \\ & + \tilde{g}_4^l(r; \omega) \int_0^r dr' \, S_{44}^l(r'; \omega) \eta_l(r', Q). \end{aligned} \tag{10}$$

The $\tilde{g}_i^l$, $i = 1, \ldots, 4$, are four linearly independent solutions of the homogeneous radial differential equation. For $r \leq R'$, the analytic solutions are given by r^l, $r^{-(l+1)}$, j_l and $h_l^{(1)}$ [17] (the $h_l^{(1)}$ are the spherical Bessel functions of the third kind). For $r > R'$, the solutions are determined by performing a numerical integration of the differential equation starting with four linearly independent initial conditions at R' (e.g. the ones determined by the values of the analytical solutions at R'). The S_{ij}^l are the matrix elements of the inverse of the 'evolution' matrix, U^l, whose columns are given by the four vectors $(\tilde{g}_i^l(r), d\tilde{g}_i^l(r)/dr, d^2\tilde{g}_i^l(r)/dr^2, d^3\tilde{g}_i^l(r)/dr^3)$, $i = 1, \ldots, 4$. The amplitudes a_l and b_l are determined by the boundary conditions at $r = R$. These are given by the continuity of $\boldsymbol{E}_\parallel$, $\boldsymbol{D}_\perp$ and $\boldsymbol{j}_\perp$. For l fixed, the third unknown in the linear system defined by the above conditions is the amplitude of the corresponding term of the potential outside the sphere, i.e. $c^l/r^{(l+1)}$. It should be noted that, in order to arrive to the expression in (10), we have used, at $r = R'$, the continuity of the same fields as above plus the continuity of ϱ/k_s^2 [18].

3. Results and comments

Our calculations were performed for an electron gas with a density corresponding to that of potassium, i.e. $r_s = 4.86\, a_0$, and for a surface diffuseness given by $R - R' = 6$ Å. (According to the local density functional results for n_0 of Lang and Kohn [16], for low-density metals, the electron 'spill' outside the ion background tends to be relatively large.) On the other hand, in the experiments reported by vom Felde *et al* the small particles are in a MgO matrix. Since this seems to cause the electrons to be compressed against the ion background [11], we have taken a rapidly decaying function to describe the ground-state electron density at the surface, namely $n_0(r) = \exp[-(r - R')^2]$, for $r > R'$. This gives a more rapid decay than in the 'free' surface results found in,

e.g. the work of Lang and Kohn for a plane surface [16] or that of Ekardt for small particles [20]. From previous studies of the hydrodynamic model [5, 8, 21], we know that it is the extension of the surface region which essentially determines the number of additional modes, while the exact eigenfrequencies are more sensitive to the rapidity of the decay of n_0. A more rapid decay shifts the modes more towards the red. In next paragraph we start the description of our results, but let us just say here that the behaviour of our spectra with varying radius and momentum transfer, which is what we concentrate on in this work, does not depend on the precise form of n_0. (This is important since in experiments one does not have perfect particles and the profiles probably change somewhat from one to another.) Following vom Felde *et al* we have also taken $\epsilon_M = 3$ as the dielectric function of the matrix. With regard to the damping factor γ, we recall that, in small particles, size effects alter considerably the value of the damping with respect to its value in the bulk. It is known that this effect can be approximately be accounted for, in the plasma frequency range, by taking $\gamma = \gamma_0 + v_F/R$ [22], where γ_0 is the inverse lifetime in the extended metal, v_F the Fermi velocity and R the particle radius. In the case of potassium, a bona fide value for γ_0 is $0.04\omega_p$. (This is a more realistic value than the one given by DC conductivity results, which is an order of magnitude lower. For a discussion on this point, see [23].)

In figure 1, we can see the energy-loss spectra (i.e. the energy-loss probability as a function of frequency) of potassium particles for three different radii and for a momentum transfer given by $q = 0.2\,\text{Å}^{-1}$. The loss probabilities $P(q,\omega)$ were divided by the particle volume and normalized to the loss probability at 6 eV. The radii are given in Å. Reasonable convergence was achieved by considering the contributions of the the l-modes up to $l = 15$. In each curve, the maximum below 2 eV is due to a superposition of the regular, or classical, surface modes of a sphere. The loss due to these modes diminishes in importance with increasing radius. The second maximum is due to the additional modes induced by surface diffuseness. Relative to the first maximum, it shows a higher contribution with increasing radius. The third mode, above 4 eV, is due to the bulk plasmon excitation. The relative intensity corresponding to this mode diminishes strongly with decreasing radius, and gives the dominant loss at large R, as one would expect. The slight red shift with increasing radius arises because in these systems, the bulk mode is not completely decoupled from the surface. With increasing radius, the 'bulk' mode relaxes towards its value for an infinite system.

In figure 2, we give the energy loss spectra of a particle with a radius of 20 Å for various values of the change in the parallel component q of the wave-vector of the scattered beam (with q given in Å^{-1}). The loss probabilities are divided by the sphere volume and normalized to the loss at 6.5 eV. The main features are the following. For low momentum transfer, the dominant loss is due to the regular surface modes, while for large q, the loss is mainly due to the bulk plasmon excitation. Moreover, the losses are more important for smaller q. The loss due to the regular modes is strongly supressed with increasing momentum transfer and shows small dispersion. The additional maximum is less suppressed with increasing q values and shows an important dispersion. This is because for higher momentum transfer, higher l modes become increasingly important, and so do their corresponding additional modes. (vom Felde *et al* arrive at a similar conclusion in their theoretical analysis, with the difference that they attribute the maximum we are considering to the classical modes of a sphere [11].) The loss intensity corresponding to the bulk mode increases with momentum

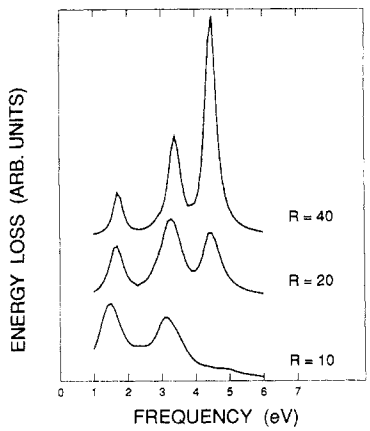

Figure 1. Energy-loss spectra of small potassium particles for three different values of the radius R (given in Å). The maxima near 1.7 eV are due to a superposition of the classical surface modes of a sphere. The modes induced by surface diffuseness give rise to the loss maxima around 3.2 eV. The bulk plasmon excitation causes the loss above 4 eV.

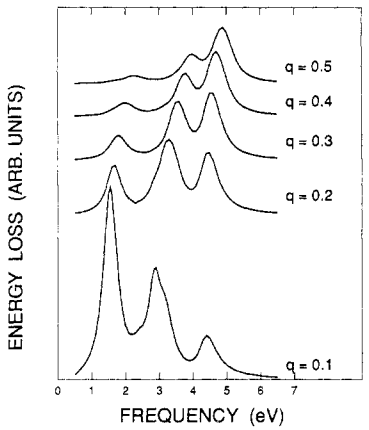

Figure 2. Energy-loss spectra for a potassium particle particle 20 Å in radius. The different curves are labelled by the change in the parallel component, q (in Å^{-1}), of the incident wavevector. The losses due to the classical, additional and bulk modes are clearly distinguishable. At low momentum transfer, the classical modes dominate, while the bulk mode dominates for high q values.

transfer up to $q \simeq 0.3\,\text{Å}^{-1}$, and then starts to diminish.

To show explicitly how the classical modes and the additional modes give rise to the structure of the EELS spectra in figures 1 and 2, we have performed a calculation of the energy loss taking $\gamma = 0.004\omega_p$, i.e. a very low inverse lifetime. In figure 3 we show the contributions of the first five l-modes, for a particle with a radius of 20 Å and for a momentum transfer corresponding to $q = 0.2\,\text{Å}^{-1}$. For comparison, the dotted line shows the corresponding result from figure 1 (for clearness, it has been displaced from the frequency axis by an arbitrary constant). One can clearly see that the classical and additional l-modes give rise, by superposition, to the two maxima below ω_p in the EELS spectra. (The maximum corresponding to $l = 1$ in the region of the classical modes is too small to be perceived.)

Let us compare now our results with the experimental curves of [11]. As in our results, the curves for particles of different radii, show the loss due to the classical modes centered around 1.7 eV. An important difference is that, what we think is the loss due to the additional mode appears around 2.5 eV (cf figure 1 of [11]), whereas in our results this loss is situated above 3 eV. This is explained by the fact that, in our treatment, the last term in (1) is a very simplified form of a quantity that should contain the spatial variation of the Fermi velocity, exchange, correlation and other effects. In the case of a plane surface, it has been shown [5] that a more consistent choice for this term pushes the additional surface plasmon to lower frequencies, yielding values that are in good agreement with the results of Dobson and Harris [24] and of Tsuei *et al* [1]. On the other hand, we cannot really understand why the experimental result for the $R = 40\,\text{Å}$ particle does not show the additional mode. Higher resolution measurements could possibly confirm its presence. With regard to the bulk mode, we see that the theoretical value lies at higher frequencies than in the experimental

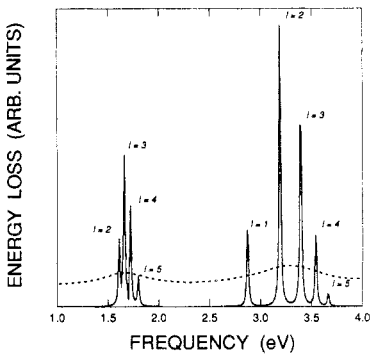

Figure 3. Contributions of the first five l-modes to the EELS spectrum using a very large value for the relaxation time ($\gamma = 0.004\omega_p$) for the $R = 20$ Å K particle and for $q = 0.2\,\text{Å}^{-1}$. For comparison, the dotted curve gives the corresponding result from figure 1. By superposition, these modes give rise to the structure observed in the EELS spectra in figures 1 and 2. (The classical $l = 1$ mode, too small to be seen, is situated at $\omega \simeq 1.5$ eV.)

curves. This is because we are using a free-electron model, and, again, exchange and correlation effects can be important in potassium due to its low density [1].

If we consider the results in [11] for different momentum transfers (cf figure 2), we see that the agreement with our calculations is very satisfying. In a calculation giving a better description of the internal kinetic energy of the electrons and further effects, the agreement would be even better since, as we explained above, the additional modes would be shifted towards the classical modes. Our curves do not show any structure around 6 eV because we have not included multiple-scattering effects in our model (the same comment is valid for our results in figure 1).

It would be very interesting to see further results on this subject, both from the experimental and theoretical points of view. One should bear in mind that the hydrodynamic approach is more qualitative than quantitative. Time-dependent density functional calculations for particles with radii higher than 10 Å—which are closer to spherical particles and in which spherical modes are probably better defined—would be necessary to give a more solid grounding to the above interpretation. The question raised here, is interesting not only on its own right, but on other grounds as well. For instance, if the existence of the additional modes in the spherical systems is confirmed, it could shed some light on some experimental results by Burtscher and Schmidt-Ott which appeared in 1982 [25]. Those workers reported a strongly enhanced van der Waals interaction among small metallic particles. To our knowledge, these results were never confirmed nor rejected. In the case of two plane surfaces, using the Casimir expression for the van der Waals interaction (i.e. in terms of the electromagnetic eigenmodes of the system [26]), it has been shown [5] that the additional mode can cause at least a four-fold enhancement of the attraction (the enhancement increases with decreasing distance between the planes). While this enhancement is not as extraordinary as that reported in [25], it points in the correct direction. On the other hand, the enhancement could be more important in the case of particles, because spheres bear not only one additional mode, but one for each value of l. These modes, moreover, should have important consequences on the optical properties of the systems we are considering, as has been shown in [8]. All these considerations, we think, show that the subject of surface modes of small particles is still open and

presents interesting problems to the theories of the inhomogeneous electron gas.

Acknowledgments

The author would like to thank P Apell, R Monreal and D Ugarte for helpful discussions concerning the subject of this article. The useful comments of the referees are also greatly acknowledged.

References

[1] Tsuei K-D, Plummer E W, Liebsch A, Kempa K and Bakshi P 1990 *Phys. Rev. Lett.* **64** 44
[2] Ritchie R H 1957 *Phys. Rev.* **106** 874
[3] Powell C J and Swan J B 1960 *Phys. Rev.* **118** 640
[4] Schwartz C and Schaich W L 1984 *Phys. Rev.* B **30** 1059
[5] Saniz R 1989 *PhD thesis* University of Geneva
[6] Levinson H J, Plummer E W and Feibelman P J 1979 *Phys. Rev. Lett.* **43** 952
Petersen H and Hagström S B M 1978 *Phys. Rev. Lett.* **41** 1314
[7] Doniach S 1984 *Proc. Conf. on Many Body Phenomena at Surfaces* ed D C Langreth and H Suhl (New York: Academic Press)
[8] Giovannini B and Saniz R 1988 *Helv. Phys. Acta* **61** 566
[9] Ganière J D, Rechsteiner R and Smithard M A 1975 *Solid State Commun.* **16** 113
Smithard M A 1973 *Solid State Commun.* **13** 153
Duthler C J, Johnson S E and Broida H P 1971 *Phys. Rev. Lett.* **26** 1236
[10] Ekardt W 1985 *Phys. Rev.* B **31** 6360
Ekardt W 1986 *Phys. Rev.* B **33** 8803
[11] vom Felde A, Fink J and Ekardt W 1988 *Phys. Rev. Lett.* **61** 2249
[12] Forstmann F and Gerhardts R R 1982 *Adv. Solid State Phys.* **22** 291
Boardman A D 1982 *Electromagnetic Surface Modes* ed A D Boardman (Chichester: Wiley)
[13] Ying S C 1974 *Nuovo Cim.* B **23** 270
Eguiluz A and Quinn J J 1976 *Phys. Rev.* B **14** 1347
[14] Fujimoto F and Komaki K 1968 *J. Phys. Soc. Japan* **25** 1679
[15] Penn D R and Apell P 1983 *J. Phys. C: Solid State Phys.* **16** 5729
[16] Lang N D and Kohn W 1970 *Phys. Rev.* B **1** 4555
[17] Tran Thoai D B and Zeitler E 1988 *Phys. Status Solidi* (a) **107** 791
[18] Arnold V 1974 *Equations Différentielles Ordinaires* (Moscow: Mir)
[19] Forstmann F and Stenschke H 1977 *Phys. Rev. Lett.* **38** 1365
[20] Ekardt W 1984 *Phys. Rev.* B **29** 1558
[21] Schwartz C and Schaich W L 1982 *Phys. Rev.* B **26** 7008
[22] Kreibig U and Fragstein C v 1969 *Z. Phys.* **224** 307
[23] Kempa K and Forstmann F 1983 *Surf. Sci.* **129** 516
[24] Dobson J F and Harris G H 1988 *J. Phys. C: Solid State Phys.* **21** L729
[25] Burtscher H and Schmidt-Ott A 1982 *Phys. Rev. Lett.* **48** 1734
[26] Casimir H B G 1948 *Proc. Kon. Ned. Akad. Wetensh.* **51** 793
Casimir H B G and Polder D 1948 *Phys. Rev.* **73** 360